Journal of Water Resources and Ocean Science
2025, Vol. 14, No. 6, pp. 163-174
https://doi.org/10.11648/j.wros.20251406.11

Research Article

Hydroclimatic Projections for the Mouhoun Basin in Burkina Faso by the Year 2100 to Support Mechanized Production Strategies

Gnirako Ahmed Donatien Bikie[1,*], Siedouba Georges Ye[2], Sie Kam[3]

[1]Physics Department, Joseph KI-ZERBO University, Ouagadougou, Burkina Faso
[2]National Center for Scientific and Technological Research (CNRST), Ouagadougou, Burkina Faso
[3]Physics Department, Joseph KI-ZERBO University, Ouagadougou, Burkina Faso

Abstract

This study assesses the potential impact of climate change on streamflow in the Mouhoun River Basin, Burkina Faso. Eight downscaled global climate models (GCMs) from CMIP6, provided by the NEX-GDDP-CMIP6 program (ACCESS-CM2, ACCESS-ESM1-5, MIROC6, MIROC-ES2L, MPI-ESM1-2-HR, MPI-ESM1-2-LR, MRI-ESM2-0, and NESM3), were employed. The ensemble mean of these models was considered for the historical period (1960–2014) and for future projections (2015–2100) under three Shared Socioeconomic Pathways (SSPs): SSP1-2.6 (optimistic), SSP2-4.5 (intermediate), and SSP5-8.5 (pessimistic). These climate data were used as inputs to the GR6J hydrological model to simulate streamflow up to 2100. The analysis focused on the interannual mean of hydro-climatic projections for three time horizons: near-term (2025–2054), mid-term (2055–2084), and long-term (2071–2100), compared with the reference period 1981–2010. Results show a general increase in streamflow across all scenarios. Under SSP1-2.6, anomalies reach +43.4% in the near term but gradually decline (+22.4% and +12.9%), indicating a tendency to return toward historical conditions. SSP2-4.5 exhibits a stronger increase (+51.2%, +36.2%, +35.3%) but also a progressive decline. In contrast, SSP5-8.5 reveals a sharp intensification of flows, with anomalies of +78.7%, +107%, and +110%, highlighting an increased risk of long-term hydrological imbalance. Regarding rainfall, an increase is observed in the northern basin under SSP1-2.6 and SSP2-4.5 (+95 mm, +60 mm, +40 mm; and +115 mm, +105 mm, +90 mm across periods), with an overall trend returning to historical levels. A similar pattern is observed in the south, with temporary increases followed by a downward trend. However, under SSP5-8.5, rainfall rises sharply in both the north (+150 mm, +210 mm, +230 mm) and the south, suggesting a sustained intensification. These results underscore the strong hydro-climatic variability across scenarios and time horizons. They highlight the urgent need for integrated water resource management strategies, particularly in the agricultural sector, to meet the growing demands of an expanding population and to mitigate risks associated with future hydrological excesses or deficits.

Keywords

Mouhoun River Basin, Streamflow, Climate Models, Hydrological Model

*Corresponding author: ahmedbikie@gmail.com (Gnirako Ahmed Donatien Bikie)

Received: 17 September 2025; **Accepted:** 21 October 2025; **Published:** 12 November 2025

1. Introduction

Assessing the potential impacts of climate change on water resources is a major challenge. Indeed, the optimal management of water resources, both in terms of quantity and quality, is a key condition for the sustainable development of any country. Such development is inevitably accompanied by increasing demands, particularly in the context of rapid population growth. In Burkina Faso, the annual population growth rate is estimated at 2.94% [1].

More than 64.8% of the Burkinabe population relies on the exploitation of natural resources for their livelihoods [1]. Currently, the riparian wetlands of the Mouhoun River in the Boromo municipality are threatened by the combined effects of climate change and anthropogenic pressure [2]. The Mouhoun River Basin is further characterized by rapid urbanization and industrial development, as well as the expansion of semi-mechanized subsistence and cash-crop agriculture [3]. Thus, in this study, the ensemble mean of eight climate models is used as input to the GR6J hydrological model in order to simulate streamflows in the Mouhoun River Basin by 2100. The simulations are conducted over three future periods (2025–2054, 2055–2070, and 2071–2100) and compared to the historical reference period (1981–2010) under three SSP scenarios. Only a few studies have applied the GR6J hydrological model in combination with SSP scenarios in Burkina Faso. The outputs of these simulations provide insights into how streamflows of the Mouhoun River at the Ouessa station may be affected by climate variability in the short, medium, and long term.

This work is the first to apply the conceptual GR6J model together with three SSP scenarios from the NEX-GDDP-CMIP6 dataset in Burkina Faso. The main objective is to simulate streamflow dynamics in order to identify future trends in the Mouhoun River Basin.

2. Materials and Methods

2.1. Study Area

The article should be written in English. An article should be between 6 and 25 pages, and exceed 2000 words. For original research articles, it should include the headings Introduction, Materials and Methods, Results, Discussion and Conclusions. Other types of articles can be written with a more flexible structure.

The study area covers five administrative regions of Burkina Faso with the following proportions: Boucle du Mouhoun (39.66%), Centre-Ouest (38.34%), Sud-Ouest (5.68%), Nord (7.15%), and Hauts-Bassins (8.84%).

The geographical location of the river outlet is situated at latitude 11.0194 ° N and longitude 2.8167 ° W, in the Ioba province, Sud-Ouest region. The relief is relatively flat, with the highest point at 570 m, the outlet at 255 m, and an average elevation of 293.61 m. The climate is classified as Sudanian-Sahelian, with annual rainfall ranging between 600 and 900 mm, characterized by the alternation of a long dry season (8 months) and a short rainy season (4 months) [3, 4].

The main river crossing the study area is the Mouhoun, a perennial river that drains the entire basin. Rainfed agriculture is predominant, with the main cereal crops being maize, rice, sorghum, and millet. The major cash crops include cotton, groundnut, bambara groundnut, sesame, cowpea, and banana. The dominant economic activities in the region are agriculture, livestock farming, and artisanal gold mining [5].

2.2. Data Collection Method

2.2.1. Observed Data

The National Meteorological Agency (ANAM) of Burkina Faso provided climatic data from fourteen stations covering the study area. These daily data consist of two synoptic stations and twelve rainfall gauges over the period 1980–2020. Specifically, they include daily rainfall for all fourteen stations, and minimum and maximum temperatures for the two synoptic stations. These observed climatic data were widely used to assess the performance of the NEX-GDDP-CMIP6 climate models.

Hydrological data for the Ouessa station were obtained from the database of the General Directorate of Water Resources of Burkina Faso (DGRE-BF). They consist of daily streamflow records covering the period 1960–2020. The climatic data (precipitation) contain few gaps, which were filled using the average rainfall from neighboring stations. The hydrological data, however, present missing values. Years with nearly complete data were selected for the calibration and validation of the GR6J hydrological model.

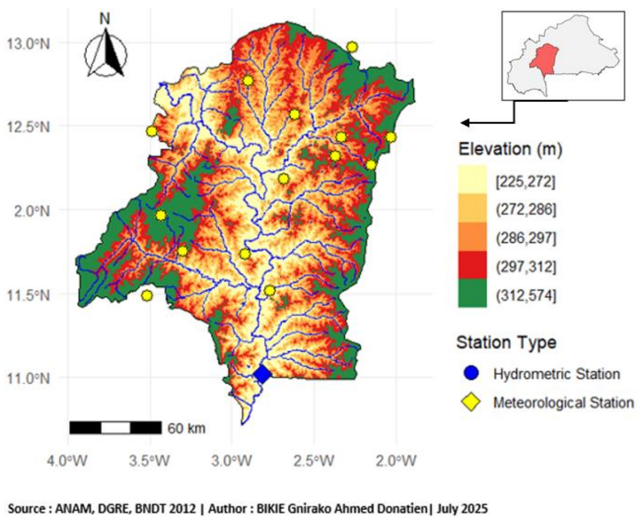

Figure 1. Upstream Lower Mouhoun Basin.

The period 1981–2010 was chosen as the historical reference for this study, as it corresponds to the climatological normal defined by the World Meteorological Organization (WMO) for a 30-year period. The spatial distribution of climatic and hydrometric stations is shown in Figure 1.

2.2.2. Climate Models

Eight climate models (Table 1) were selected from the Shared Socioeconomic Pathways (SSPs), which represent alternative development trajectories for future societies under climate change and related policies. These scenarios can also support the design of mechanized agricultural production models adapted to Burkina Faso, similar to approaches already tested in Niger [6].

In this study, three SSPs were considered: the optimistic scenario (SSP1-2.6), the intermediate scenario (SSP2-4.5), and the pessimistic scenario (SSP5-8.5). The selection was motivated by the fact that the NEX-GDDP-CMIP6 dataset is the latest version of the NASA Earth Exchange Global Daily Downscaled Projections, providing daily climate projections at a high horizontal resolution of 0.25° (~25 km) [7]. The spatial resolution of the selected models is presented in Table 1.

Table 1. *Climate models used.*

N°	Modeling Center	Parameters				Spatial Resolution
		Precipitation (mm)	Minimal temperature (°C)	Maximale température (°C)	Radiation W/m²	(lat x lon)
1	Australian Community Climate and Earth-System Simulator – Climate Model version 2	pr	tasmin	tasmax	rsds	0,25 x 0,25
2	Australian Community Climate and Earth-System Simulator – Earth System Model version 1.5	pr	tasmin	tasmax	rsds	0,25 x 0,25
3	Model for Interdisciplinary Research on Climate version 6	pr	tasmin	tasmax	rsds	0,25 x 0,25
4	Model for Interdisciplinary Research on Climate – Earth System version 2 for Long-term simulations	pr	tasmin	tasmax	rsds	0,25 x 0,25
5	Max Planck Institute Earth System Model version 1.2 – High Resolution	pr	tasmin	tasmax	rsds	0,25 x 0,25
6	Max Planck Institute Earth System Model version 1.2 – Low Resolution	pr	tasmin	tasmax	rsds	0,25 x 0,25
7	Meteorological Research Institute Earth System Model version 2.0	pr	tasmin	tasmax	rsds	0,25 x 0,25
8	Nanjing University of Information Science and Technology Earth System Model version 3	pr	tasmin	tasmax	rsds	0,25 x 0,25

2.3. Methods

2.3.1. Calculation of Spatial Average of Climate Parameters

The aim is to determine the annual average of precipitation and temperatures by considering observations from the fourteen stations using well-established methods in the literature. The same approach is applied to climate model outputs (0.25° grid resolution), where the spatial average over the study area is calculated. These average values are then used to evaluate the performance of the simulations and to represent the temporal evolution of the parameters graphically.

For observed precipitation, the annual rainfall at the watershed scale was estimated using the Thiessen polygon method [8]. For observed maximum and minimum temperatures at the two synoptic stations, kriging interpolation was applied to determine the spatially averaged temperature over the study area [9].

For simulated data, a spatially weighted average based on the surface area of grid cells intersecting the watershed was used to calculate the mean precipitation from each climate model. The multi-model average was then computed for the different periods considered.

2.3.2. Evaluation of Climate Models

The adopted methodology first involved the validation of the eight NEX-GDDP-CMIP6 climate models. The ensemble mean of these eight models was then used as input for the hydrological model to simulate streamflow. The Root Mean Square Error (RMSE) and the percentage bias (%Bias) were used to evaluate the performance of each climate model compared to observed data. The climate parameters considered for these tests included precipitation, minimum, and maximum temperatures.

Averaging across multiple models reduces uncertainties inherent to individual models and enhances the robustness of projections [10]. Using this multi-model ensemble, climate projections up to 2100 were determined. RMSE measures the absolute error of the climate model in simulating a given climate variable. Lower RMSE values indicate better model performance, and vice versa [11]. RMSE is defined as follows:

$$\text{RMSE} = \sqrt{\frac{1}{n}\sum_{i=1}^{n}\left(P_{jr,i}^{sim} - P_{jr,i}^{obs}\right)^2} \quad (1)$$

Where

$P_{jr,i}^{sim}$: Simulated daily rainfall on day i

$P_{jr,i}^{obs}$: Observed daily rainfall on day i

n: Total number of days in the considered series

The PBIAS measures the average tendency of the simulated data relative to the observed data. Positive values indicate underestimation, while negative values indicate overestimation by the climate model. The optimal PBIAS value is 0. Values close to 0 indicate very good simulation accuracy [11, 12]. Its formula is:

$$\text{PBIAS} = \frac{\sum_{i=1}^{n}\left(\overline{X_{sim}} - \overline{X'_{obs}}\right)}{\sum_{i=1}^{n}\overline{X'_{obs}}} \quad (2)$$

Where

$\overline{X_{sim}}$: Mean of the simulated parameters (precipitation, temperature)

$\overline{X'_{obs}}$: Mean of the observed parameters (precipitation, temperature)

2.3.3. Annual Rainfall Analysis

An analysis of the annual rainfall evolution was conducted to determine the trends and anomalies of the projections for each scenario relative to the historical reference period. Annual rainfall at the watershed scale, based on the fourteen stations, was estimated using the Thiessen polygon method [8]. For observed temperatures (maximum and minimum) at the stations, the kriging interpolation method was applied to estimate the average temperature [9] at the study area scale. A spatially weighted mean, based on the area of the grid cells intersecting the watershed, was used to determine the average precipitation from the simulated data, considering the multi-model mean for the different periods.

2.3.4. Calibration and Validation of the GR6J Hydrological Model

The outputs of the multi-model ensemble and observed data were used as inputs to the hydrological model to simulate streamflow for different periods. Precipitation and potential evapotranspiration (PET) were used as input data. A spatially weighted mean, based on the area of the grid cells intersecting the watershed, was used to calculate the average values of minimum and maximum temperatures and PET at the study area scale.

Evapotranspiration data were calculated using the Hargreaves formula from the mean values of minimum and maximum temperatures and solar radiation. The modified Hargreaves-Samani formula [13] was used to compute potential evapotranspiration, given by the following equation:

$$\text{ETPHS} = 0{,}0023 \times (\text{Tmean} + 17{,}8) \times \sqrt{\text{Tasmax} - \text{Tasmin}} \times \text{Rsds} \quad (3)$$

Where

$\text{Tmean} = \frac{\text{Tmin}+\text{Tmax}}{2}$ is the daily mean temperature.

Tasmax et Tasmin are the daily maximum and minimum temperatures.

Rsds is the daily solar radiation received at the ground, expressed in w/m ²/day of equivalent evapotranspiration.

The GR6J model was calibrated over the period 1970–1975 using observed data to evaluate the model's performance in simulating streamflows. For validation, future flow simulations for 2012–2014 were conducted using the calibration parameter sets. Three quantitative criteria were used to assess the performance of the GR6J model during calibration and validation:

1) the Nash–Sutcliffe efficiency (NSE) [14], commonly used in hydrology and based on the sum of squared errors;
2) the percent bias (PBIAS), which measures the relative difference between simulated and observed volumes, thus evaluating whether the model systematically overestimates or underestimates flows;
3) the Pearson correlation coefficient (R), which measures the strength and direction of a linear relationship between two continuous quantitative variables, ranging from –1 to +1.

The calibration parameters were then used to simulate streamflows from 2015 to 2100 and to fill gaps in the reference period. The dimensionless and normalized statistic called the Nash–Sutcliffe efficiency (NSE) indicates the extent to which residual variation is important relative to the variance of the observed data. The NSE can be calculated using the following equation:

$$NSE = 1- \frac{\sum_{i=1}^{n}(Q_i - Q_i')^2}{\sum_{i=1}^{n}(Q_i - \bar{Q})^2} \tag{4}$$

Where Qi and Qi′are the observed and simulated flows at the iii-th observation, respectively; $\bar{Q}$ is the mean of the observed flows over the simulation period.

The ideal value of NSE is 1.

$$PBIAIS = \frac{\sum_{i=1}^{n}(Q_i - Q_i')}{\sum_{i=1}^{n} Q_i'} \tag{5}$$

Q_i = Simulated daily streamflow at the i observation;

Q_i' = Observed daily streamflow at the i observation.

n: Total number of days in the considered series.

The Pearson correlation coefficient is determined using the following relation:

$$R = \frac{\sum_{i=1}^{n}(Qobs,i-\overline{Qobs})(Qsim,i-\overline{Qsim})}{\sqrt{\sum_{i=1}^{n}(Qobs,i-\overline{Qobs})^2}\sqrt{\sum_{i=1}^{n}(Qsim,i-\overline{Qsim})^2}} \tag{6}$$

Where Qobs,i = observed value at time i; Qsim, = simulated value at time i; $\overline{Qobs}$ = mean of observed values; $\overline{Qsim}$ = mean of simulated values; n = total number of observations. R=1 or −1 corresponds to a perfect correlation (positive or negative). In general, NS>0.50 and ∣PBIAS∣<25% are used as criteria for satisfactory simulations in hydrological modeling. When NS>0.75 and ∣PBIAS∣<10%, the simulation is considered very good [15]. In hydrology, a correlation coefficient R≥0.7 is usually regarded as indicating a strong relationship between simulated and observed streamflows.

2.3.5. Streamflow Analysis

This analysis consists of plotting the flood hydrograph for the three time horizons (short-term, medium-term, and long-term) relative to the historical period (1981–2010) under the three SSP scenarios. This representation allows the interpretation of anomalies (in percentage) between periods in order to better assess future runoff trends. All operations were carried out using R Studio software.

3. Results

3.1. Validation of Climate Models

For precipitation, we observe that the RMSE ranges between 5 and 10 mm for the period 1980–2014. The percentage bias varies between 6% and 15% for the same period. Overall, these values are considered satisfactory (Table 2).

Table 2. *Historical precipitation data.*

N°	Models	Period	RMSE	% Piais
1	ACCESS-CM2	1980-2014	5,424	10,163
2	ACCESS-ESM1-5	1980-2014	5,434	10,162
3	MIROC6	1980-2014	5,654	6,25
4	MIROC-ES2L	1980-2014	5,5	6,925
5	MPI-ESM1-2-HR	1980-2014	5,299	11,339
6	MPI-ESM1-2-LR	1980-2014	10,386	5,433
7	MRI-ESM2-0	1980-2014	5,77	9,041
8	NESM3	1980-2014	5,593	15,261

We observe that for maximum temperature, the RMSE is around 3 degrees for the period 1980 to 2014. The percentage bias ranges between -1% and -2% for the same period. These values are generally good.

Table 3. *Historical maximum temperature data.*

N°	Models	Period	RMSE	% Piais
1	ACCESS-CM2	1980-2014	3,115	-1,439
2	ACCESS-ESM1-5	1980-2014	3,066	-1,475
3	MIROC6	1980-2014	3,154	-1,742
4	MIROC-ES2L	1980-2014	3,026	-1,652
5	MPI-ESM1-2-HR	1980-2014	3,12	-2,004
6	MPI-ESM1-2-LR	1980-2014	3,033	-1,767
7	MRI-ESM2-0	1980-2014	3,075	-1,79
8	NESM3	1980-2014	3,06	-2,431

For minimum temperature, the RMSE ranges between 2 and 3 ℃ for the period 1980–2014. The percentage bias varies between 0% and -1% over the same period. Overall, these values are considered satisfactory.

Table 4. *Historical minimum temperature data.*

N°	Models	Period	RMSE	% Piais
1	ACCESS-CM2	1980-2014	2,947	-0,834
2	ACCESS-ESM1-5	1980-2014	2,911	-0,445
3	MIROC6	1980-2014	2,544	-1,053
4	MIROC-ES2L	1980-2014	2,582	-1,068
5	MPI-ESM1-2-HR	1980-2014	3,203	-1,248
6	MPI-ESM1-2-LR	1980-2014	3,015	-1,119
7	MRI-ESM2-0	1980-2014	2,825	-1,038
8	NESM3	1980-2014	3,166	-1,222

3.2. Performance of the Hydrological Model During Calibration and Validation

Table 2 provides a summary of the results obtained during the calibration and validation phases. Overall, the Nash–Sutcliffe efficiency (NSE) and percent bias (PBIAS) values during validation are generally acceptable. For the calibration and validation periods, the NSE values are 0.607 and 0.524, respectively. Regarding PBIAS, the values are –0.26 and –14.38. The correlation coefficient (R) is 0.78 for calibration and 0.786 for validation. The parameter values (X1, X2, X3, X4, X5, and X6) obtained are then used for the simulation of future streamflows.

Table 5. *Performance of the GR6J model during calibration and validation.*

	Period	Nash–Sutcliffe Efficiency (NSE) (%)	Percentage Bias (PBIAS)	Pearson correlation coefficient R
Calibration	1971-1975	0,607	-0.26	0,78
Validation	2012-2014	0,524	-14,38	0,786

3.3. Evolution of Annual Rainfall up to 2100

Figure 2 presents a line graph illustrating annual rainfall, obtained from the average of eight climate models. The historical multi-model data cover the period 1960–2014, which serves as the reference dataset for the model. Future projections from 2015 to 2100 were generated for the SSP1-2.6, SSP2-4.5, and SSP5-8.5 scenarios. A rising trend in annual rainfall is observed during the historical period. For the projections, the SSP5-8.5 scenario predicts an increasing trend in annual rainfall, while the SSP1-2.6 and SSP2-4.5 scenarios indicate a decreasing trend despite positive anomalies (Figure 2). The anomalies for the three projection periods (short-term, medium-term, and long-term) relative to the historical period are shown in Figure 3. For the SSP1-2.6 scenario, the average annual rainfall is projected to increase by 95 mm, 60 mm, and 40 mm in the northern part for the three periods compared to the reference historical period, although a decreasing trend is noted. In the southern part, increases of 40 mm, 40 mm, and 25 mm are observed, also followed by a declining trend. Under the SSP2-4.5 scenario, the northern region is expected to see increases of 115 mm, 105 mm, and 90 mm, while the southern region shows increases of 80 mm, 60 mm, and 65 mm, again with a decreasing tendency. For the SSP5-8.5 scenario, the northern part exhibits substantial increases of 150 mm, 210 mm, and 230 mm across the three periods, whereas the southern region experiences decreases of 100 mm, 125 mm, and 120 mm relative to the historical reference period, indicating an overall upward trend in rainfall.

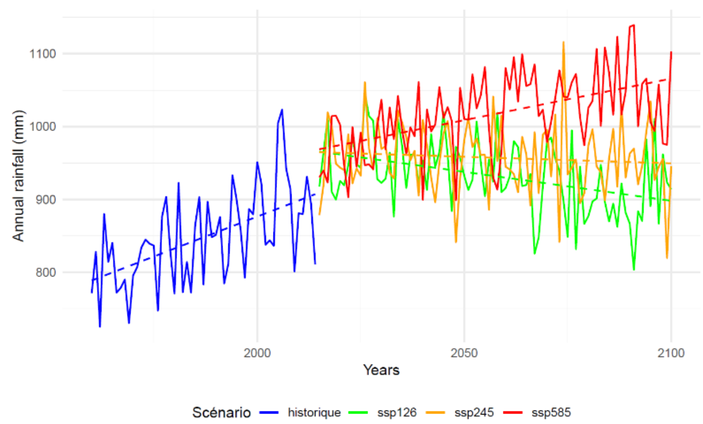

Figure 2. *Evolution of annual rainfall up to 2100 under three SSP scenarios from 2015 to 2100 relative to the historical reference period 1960–2014.*

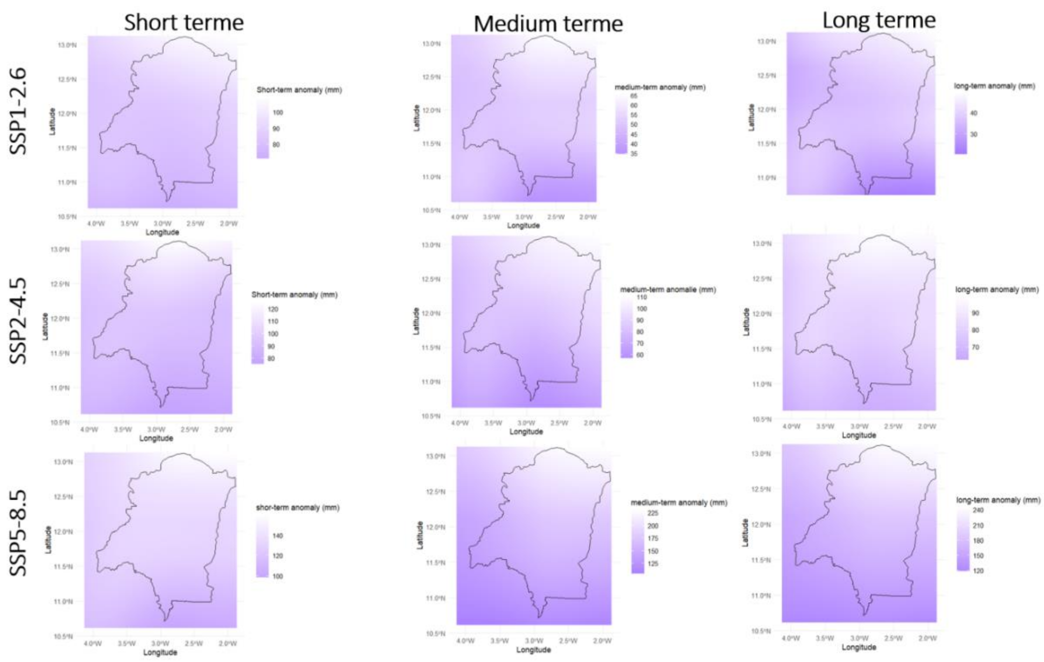

Figure 3. *Short-term, medium-term, and long-term anomalies of the scenarios relative to the historical period.*

3.4. Evolution of Streamflow Through 2100

Figure 4 presents the projected mean monthly river discharge for the SSP1-2.6, SSP2-4.5, and SSP5-8.5 scenarios over three future periods compared to the historical period. The maximum discharge occurs in September for all four periods (1981–2010, 2025–2054, 2055–2084, and 2071–2100) across all scenarios. Hydrological projections indicate an overall increase in simulated mean flows for the short, medium, and long term. In the short term (2025–2054), anomalies reach +43.4% (SSP1-2.6), +51.2% (SSP2-4.5), and +78.7% (SSP5-8.5). In the medium term (2055–2084), anomalies range between +22.4%, +36.2%, and +107%. For the long term (2071–2100), they vary from +12.9% and +35.3% up to a maximum of +110% under SSP5-8.5.

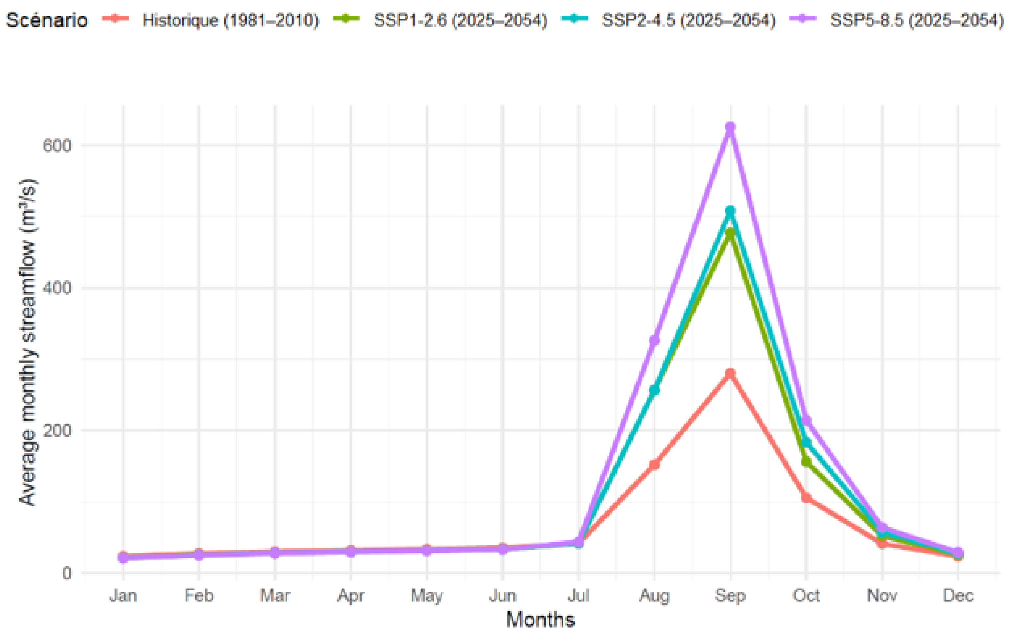

Short term

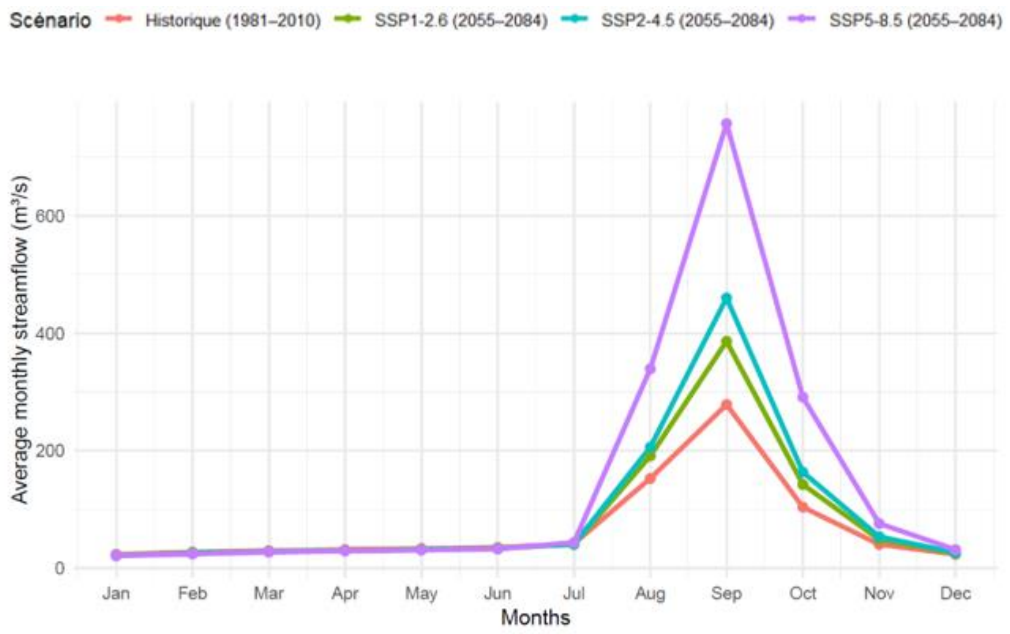

Middle term

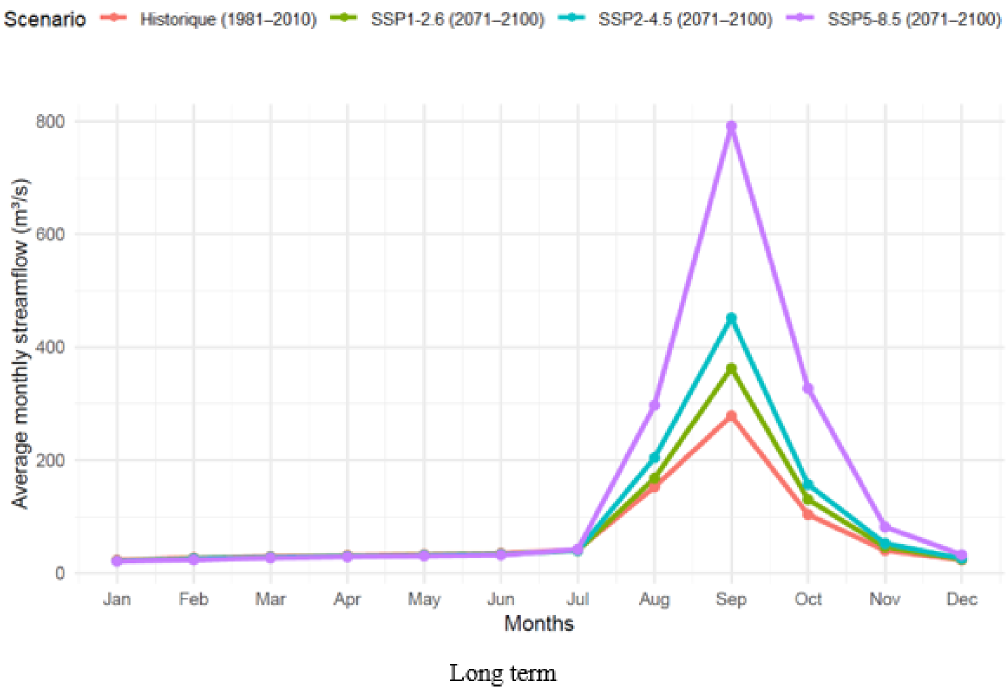

Figure 4. *Evolution of Mouhoun River Flows through 2100 (2025–2054, 2055–2084, and 2071–2100) Compared to the Historical Period (1981–2010) under Three SSP Scenarios.*

4. Discussion

In recent years, the Mouhoun sub-basin has faced multiple challenges due to intensified human activities, such as water abstraction for agricultural and industrial purposes, urbanization, and industrialization [3]. These activities can lead to soil erosion, loss of forest cover, and degradation of water quality. Moreover, climate change is expected to further impact the sub-basin by altering rainfall patterns and increasing the frequency and intensity of extreme weather events.

In this study, the average of eight NEX-GDDP-CMIP6 climate models was used as input data to simulate the hydrological behavior of the basin, producing acceptable results despite uncertainties at some observation stations. Model validation was performed using RMSE and percent bias, and the multi-model mean was applied. The GR6J hydrological model was used to simulate river flows at the Ouessa station. Model performance was assessed using metrics such as the Nash-Sutcliffe Efficiency (NSE) and percent bias. The conceptual model used precipitation and evapotranspiration (ETP) as input, with ETP derived from maximum and minimum temperatures and solar radiation. Model parameter optimization was performed using the L-BFGS-B algorithm, a constrained quasi-Newton method suitable for nonlinear hydrological models with a limited number of parameters [16].

The results indicate that the GR6J model demonstrated acceptable performance in simulating daily flows, both in calibration and validation, despite missing daily observations at the Ouessa station. Only periods with sufficient data were used for calibration and validation. During calibration, the model achieved an NSE of 0.607, percent bias of −0.26, and a Pearson correlation coefficient of 0.78. For validation, NSE was 0.524, percent bias −14.38, and Pearson correlation 0.786. Overall, GR6J effectively fitted observed flow data and predicted flows for independent datasets. It should be noted that the calibration period covers 1971–1975, while the validation period spans 2012–2014. These periods were selected because they contain the fewest gaps in the entire observation series obtained from the General Directorate of Water Resources. A longer continuous dataset without gaps, compared to the one we considered, would provide even more robust results and further reduce model uncertainties.

Annual precipitation forecasts for the historical period and three SSP scenarios (SSP1-2.6, SSP2-4.5, SSP5-8.5) were analyzed. The SSP5-8.5 scenario showed the most significant changes across all projection periods compared to the reference historical period. In the northern part of the basin, annual rainfall is projected to increase markedly under all three scenarios. For SSP1-2.6 and SSP2-4.5, an upward trend is also observed, though smaller than that under SSP5-8.5.

Regarding river flows, monthly mean discharge projections under the three scenarios were analyzed relative to the historical period. Peak flows consistently occur in September across all periods (1981–2010, 2025–2054, 2055–2084, and 2071–2100), indicating that September will continue to experience maximum flows at the basin outlet. Farmers in the study area should remain vigilant during this month to prevent potential damage. In the short term, all scenarios predict a significant increase in flows, reflecting an intensification of the hydrological cycle. This increase is particularly pronounced under SSP5-8.5, with anomalies reaching +78.7%. In the medium and long term, trends decrease for SSP1-2.6 and SSP2-4.5, while anomalies under SSP5-8.5 reach +110%, indicating a high risk of extreme flows. Overall, all scenarios indicate a general upward trend in river discharge, with the magnitude of change strongly scenario-dependent and most pronounced under SSP5-8.5.

Possible contributing factors include changes in rainfall patterns, land use, and water management practices in the region. A study in the Massili sub-basin of the Nakambé reported a 95.76% variation in flows between 1975–2002 and 2003–2019 [17]. Between 2011 and 2040, models METO-HC and GKSS-CCLM4 projected a 22% increase in annual mean flows [18]. In the Kou sub-basin of the Mouhoun, 74% of the basin is at risk of flooding [19]. Similarly, in the Dano sub-basin, comparing projected flows (2021–2050) to a reference period (1971–2000) showed substantial uncertainty among regional climate models, with some predicting increases of +12% to +95%, and others decreases of −44% to −24% [20]. According to the Master Plan for Water Management in the Mouhoun Basin (SDAGE 2014–2030), seasonal flows may decrease during the dry season (January–July) by 23–46 million m^3 (~1%), compensated by increases during the rainy season (August–October). In general, small and medium basins in the Sahelian zone show increasing flows, while the Sudanese-Guinean zone shows decreasing trends, a phenomenon termed the “Sahelian paradox” [21].

These trends may increase the frequency of flooding in agricultural areas, potentially reducing crop yields and prompting population migration to more favorable areas. To mitigate these impacts while optimizing yields, measures such as constructing earth and stone dikes for soil conservation [22], prioritizing early-maturing crops, diversifying crops, and implementing agroforestry [23] are recommended.

5. Conclusion

This study assessed the potential impacts of climate change on flows in the Mouhoun Basin using a combination of eight NEX-GDDP-CMIP6 climate models and the GR6J hydrological model. The multi-model mean was used to simulate flows. Results indicate a general increase in future flows across short-, medium-, and long-term periods, with particularly high levels under the pessimistic SSP5-8.5 scenario. Peak flows consistently occur in September across all periods. Precipitation analysis shows increased cumulative rainfall in some areas, but a decreasing trend for moderate scenarios, highlighting enhanced hydro-climatic variability. These projected flow trends align with observed annual rainfall trends across the three scenarios.

However, these results should be interpreted with caution due to gaps in observed hydrometric data, which may introduce uncertainties in hydrological modeling.

Abbreviations

ANAM	National Meteorological Agency
DGRE	General Directorate of Water Resources of Burkina Faso
ETP	Potential Evapotranspiration
Pr	Precipitation
Rsds	Radiation
Tasmin	Minimum Temperature
Tasmax	Maximum Temperature
Tmean	Mean Temperature

Acknowledgments

The author would like to thank the National Meteorological Agency and the General Directorate of Water Resources of Burkina Faso for providing access to the rainfall, temperature and Streamflow dataset.

Author Contributions

Gnirako Ahmed Donatien Bikie: Conceptualization, Data curation, Formal Analysis, Funding acquisition, Methodology, Resources, Validation, Writing – original draft, Writing – review & editing

Siedouba Georges Ye: Conceptualization, Data curation, Formal Analysis, Investigation, Methodology, Project administration, Supervision, Validation, Visualization, Writing – review & editing

Sie Kam: Conceptualization, Data curation, Formal Analysis, Methodology, Project administration, Supervision, Validation, Visualization, Writing – review & editing

Funding

This work is not supported by any external funding.

Data Availability Statement

The data that support the findings of this study can be found at the National Meteorological Agency and the General Directorate of Water Resources of Burkina Faso. Climate data that support the findings of this study can be found at: https://esgf-data.dkrz.de/search/cmip6-dkrz/

Conflicts of Interest

The authors declare no conflicts of interest.

References

[1] INSD, « gph 2019 burkina faso pdf - Google search ». Viewed on: 15th February 2025. [Online]. Available on: https://www.insd.bf/fr/file-download/download/public/2071

[2] A. A. Sodere, O. Blaise, O. Aboubacar, et R. Noel, « THE RAMSAR SITES OF THE BOUCLE DU MOUHOUN FOREST CORRIDOR IN BURKINA FASO, BETWEEN SECTORAL MANAGEMENT AND THE SEARCH FOR SYNERGY OF ACTION THE RAMSAR SITES OF THE BOUCLE DU MOUHOUN FOREST CORRIDOR IN BURKINA FASO, BETWEEN SECTORAL MANAGEMENT AND THE SEARCH FOR SYNERGY OF ACTION ». Viewed on: 8th July 2025. [Online]. Available on: https://www.researchgate.net/publication/351271744_LES_SITES_RAMSAR_DU_CORRIDOR_FORESTIER_DE_LA_BOU-CLE_DU_MOUHOUN_AU_BURKINA_FASO_ENTRE_GES-TION_SECTORIELLE_ET_RECHERCHE_DE_SYNERGIE_D'ACTION_THE_RAMSAR_SITES_OF_THE_BOUCLE_DU_MOUHOUN_FOREST_CORRIDOR_IN_

[3] H. OUEDRAOGO, B. J.-B. ZOUNGRANA, J. ROUAMBA, et G. ZONGO, « Influence of land use dynamics on the Mouhoun River in Burkina Faso », Rev. Int. Cherch., vol. 5, no 1, 2024, Viewed on: 8th july 2025. [Online]. Available on: https://revuechercheur.com/index.php/home/article/view/902

[4] G. A. D. Bikie, S. G. Ye, T. P. Bonthogo, U. Diasso, et S. Kam, « Pluviometric variability of the Mouhoun Basin in Burkina Faso from 1980 to 2020 », Glob. NEST J., avr. 2025, https://doi.org/10.30955/gnj.06700

[5] B. J.-B. ZOUNGRANA, « Trends in vegetation cover in the riparian wetland area of the Mouhoun River in Boromo, Burkina Faso », Rev. Int. Cherch., vol. 5, no 4, 2024, Viewed on: 8th july 2025. [Online]. Available on: https://www.revuechercheur.com/index.php/home/article/view/1192

[6] F. Röhrig et al., « Climate Risk Analysis for Identifying and Weighing Adaptation Strategies in Niger's Agricultural Sector », 2021, https://doi.org/10.48485/pik.2022.002

[7] B. Thrasher, W. Wang, A. Michaelis, F. Melton, T. Lee, et R. Nemani, «NASA global daily downscaled projections, CMIP6 », Sci. Data, vol. 9, no 1, p. 262, 2022. https://www.nature.com/articles/s41597-022-01393-4

[8] A. I. Chowdhury, M. M. Kabir, A. F. Sayed, et S. Hossain, « Estimation of rainfall patterns in Bangladesh using different computational methods (arithmetic average, thiessen polygon and isohyet) », 2016. https://www.researchgate.net/profile/Md-Ashraful-Chowdhury/publication/309935619_Assessment_of_river_encroachment_and_land-use_patterns_in_Dhaka_city_and_its_peripheral_rivers_using_GIS_techniques/links/6083f21e907dcf667bbdfe66/Assessment-of-river-encroachment-and-land-use-patterns-in-Dhaka-city-and-its-peripheral-rivers-using-GIS-techniques.pdf

[9] T. FOWE, J.-E. PATUREL, et H. KARAMBIRI, « Impacts of global changes on water resources in the Sahel region of West Africa », IAHS-AISH Publ., vol. 359, p. 99-104, 2013. https://www.researchgate.net/profile/Tazen-Fowe/publication/273758620_Impacts_des_changements_globaux_sur_les_ressources_en_eau_dans_la_zone_sahelienne_en_Afrique_de_l'Ouest/links/550aa3110cf265693ced686a/Impacts-des-change-ments-globaux-sur-les-ressources-en-eau-dans-la-zone-sahelienne-en-Afrique-de-lOuest.pdf

[10] H. Daniel, « Performance assessment of bias correction methods using observed and regional climate model data in different watersheds, Ethiopia », J. Water Clim. Change, vol. 14, no 6, p. 2007-2028, june 2023, https://doi.org/10.2166/wcc.2023.115

[11] C. D. Geleta et L. Gobosho, « Climate change induced temperature prediction and bias correction in Finchaa watershed », Agric Env. Sci, vol. 18, p. 324-337, 2018. https://www.researchgate.net/profile/Leta-Ameja/publication/362469576_Climate_Change_Induced_Temperature_Predic-tion_and_Bias_Correction_in_Finchaa_Watershed/links/62ebaaf988b83e7320aa1123/Climate-Change-Induced-Temperatu-re-Prediction-and-Bias-Correction-in-Finchaa-Watershed.pdf

[12] G. H. Fang, J. Yang, Y. N. Chen, et C. Zammit, « Comparing bias correction methods in downscaling meteorological variables for a hydrologic impact study in an arid area in China », Hydrol. Earth Syst. Sci., vol. 19, no 6, p. 2547-2559, 2015. https://hess.copernicus.org/articles/19/2547/2015/

[13] N. A. Elagib et A. A. Musa, « Correcting Hargreaves-Samani formula using geographical coordinates and rainfall over different timescales », Hydrol. Process., vol. 37, no 1, p. e14790, 2023, https://doi.org/10.1002/hyp.14790

[14] J. E. Nash et J. V. Sutcliffe, « River flow forecasting through conceptual models part I—A discussion of principles », J. Hydrol., vol. 10, no 3, p. 282-290, 1970.

[15] D. N. Moriasi, J. G. Arnold, M. W. Van Liew, R. L. Bingner, R. D. Harmel, et T. L. Veith, « Model evaluation guidelines for systematic quantification of accuracy in watershed simulations », Trans. ASABE, vol. 50, no 3, p. 885-900, 2007. https://elibrary.asabe.org/abstract.asp?aid=23153

[16] D. R. S. Saputro et P. Widyaningsih, « Limited memory Broyden-Fletcher-Goldfarb-Shanno (L-BFGS) method for the parameter estimation on geographically weighted ordinal logistic regression model (GWOLR) », in AIP conference proceedings, AIP Publishing LLC, 2017, p. 040009. Viewed on: 27 th july 2025. [Online]. Available on: https://pubs.aip.org/aip/acp/article-abstract/1868/1/040009/641492

[17] B. M. Philippe, Y. Roland, S. B. Abdoulaye, et S. Y. S. Corenthin, « Impact of land use changes on flow rates in the Massili watershed in Gonsé (Burkina Faso) », VertigO - Rev. Électronique En Sci. Environ., no 23-1, Art. no 23-1, avr. 2023, https://doi.org/10.4000/vertigo.39765

[18] T. FOWE, K. HAROUNA, Y. HAMMA, et B. BRUNO, « IMPACT OF CLIMATE AND LAND USE SCENARIOS ON WATER RESOURCES IN THE NAKANBE RIVER BASIN (BURKINA FASO) », 2012, Viewed on: 9 juillet 2025. [Online]. Available on: https://www.researchgate.net/profile/Tazen-Fowe/publication/251230558_Impacts_des_scenarii_climatiques_et_de_l'occupation_des_sols_sur_les_ressources_en_eau_du_bassin_versant_du_Nakanbe_Burkina_Faso/links/550aa1690cf29e53c80bc8fb/Impacts-des-scenarii-climatiques-et-de-loccupation-des-sols-sur-les-ressources-en-eau-du-bassin-versant-du-Nakanbe-Burkina-Faso.pdf

[19] S. Guelbeogo et L. Ouédraogo, « Flood risk mapping in the Kou river basin in Burkina Faso », Afr Sci, vol. 21, p. 60-75, 2022. https://www.afriquescience.net/admin/postpdfs/e9990d89ca25b083991746d0390d0fed1719901097.pdf

[20] M. Idrissou et al., « Modeling the Impact of Climate and Land Use/Land Cover Change on Water Availability in an Inland Valley Catchment in Burkina Faso », Hydrology, vol. 9, no 1, Art. no 1, janv. 2022, https://doi.org/10.3390/hydrology9010012

[21] L. Descroix et al., « Paradoxes and contrasts in West Africa: climatic and anthropogenic impacts on runoff », 2019. https://ird.hal.science/ird-02153159/document

[22] M. E. Adamseged et S. W. Kebede, « Are farmers' climate change adaptation strategies understated? Evidence from two communities in northern Ethiopian highlands », Clim. Serv., vol. 30, p. 100369, 2023. https://www.sciencedirect.com/science/article/pii/S2405880723000304

[23] S. Eswaran et al., « Climate Change Impacts on Agricultural Systems Mitigation and Adaptation Strategies: A Review », J. Exp. Agric. Int., vol. 46, no 11, p. 1-12, nov. 2024, https://doi.org/10.9734/jeai/2024/v46i113021